

Relative Spectra and Distributions of Fluences of ^3He and ^4He in Solar Energetic Particles

Vahé Petrosian^{1,2,3}, Yan Wei Jiang^{1,2}, Siming Liu⁴, George C. Ho⁵ and Glenn, M. Mason⁵

ABSTRACT

Solar Energetic Particles (SEPs) show a rich variety of spectra and relative abundances of many ionic species and their isotopes. A long standing puzzle has been the extreme enrichments of ^3He ions. The most extreme enrichments are observed in low fluence, the so-called impulsive, events which are believed to be produced at the flare site in the solar corona with little scattering and acceleration during transport to the Earth. In such events ^3He ions show a characteristic concave curved spectra in a log-log plot. In two earlier papers (Liu et al. 2004 and 2006) we showed how such extreme enrichments and such spectra can result in the model developed by Petrosian & Liu (2004), where ions are accelerated stochastically by plasma waves or turbulence. In this paper we address the relative distributions of the fluences of ^3He and ^4He ions presented by Ho et al. (2005) which show that while the distribution of ^4He fluence (which we believe is a good measure of the flare strength) like many other extensive characteristics of solar flare, is fairly broad, the ^3He fluence is limited to a narrow range. Moreover, the ratio of the fluences shows a strong correlation with the ^4He fluence. One of the predictions of our model presented in the 2006 paper was presence of steep variation of the fluence ratio with the level of turbulence or the rate of acceleration. We show here that this feature of the model can reproduce the observed distribution of the fluences with very few free parameters. The primary reason for the success of the model in both fronts is because fully ionized ^3He ion, with its unique charge to mass ratio, can resonantly interact with more plasma modes and accelerate more readily than ^4He . Essentially in most flares,

¹Department of Physics, Stanford University, Stanford, CA, 94305 email; vahep@stanford.edu; ar-jiang@stanford.edu

²Kavli Institute for Particle Astrophysics and Cosmology, Stanford University, Stanford, CA 94305

³Also Department of Applied Physics

⁴Los Alamos National Laboratory, Los Alamos, NM, 87545

⁵Applied Physics Laboratory, Johns Hopkins University, 11100 Johns Hopkins Road, Laurel, MD 20723

all background ^3He ions are accelerated to few MeV/nucleon range, while this happens for ^4He ions only in very strong events. A much smaller fraction of ^4He ions reach such energies in weaker events.

Subject headings: Sun: flares, particle emissions – acceleration–plasmas – turbulence–waves

1. INTRODUCTION

Solar flares are excellent particle accelerators. Some of these particles on open field lines are observed as solar energetic particles (SEPs) at one AU or produce type III and other radio radiation. Those on closed field lines can be observed by the radiation they produce as they interact with solar plasma and fields. Electrons produce nonthermal bremsstrahlung and synchrotron photons in the hard X-ray and microwave range, while protons (and other ions) excite nuclear lines in the 1 to 7 MeV range or may produce higher energy gamma-rays via π^0 production and its decay. It appears that stochastic acceleration (SA) of particles by plasma waves or turbulence plays an important role in production of high energy particles and consequent plasma heating in solar flares (e.g., Ramaty 1979; Möbius et al. 1980, 1982; Hamilton & Petrosian 1992; Miller et al. 1997; Petrosian & Liu 2004, hereafter PL04). This theory was applied to the acceleration of nonthermal electrons (Miller & Ramaty 1987; Hamilton & Petrosian 1992). It appears that it can produce many of the observed radiative signatures such as broad band spectral features (Park, Petrosian & Schwartz 1997; PL04) and the commonly observed hard X-ray emission from the tops of flaring loops (Masuda et al. 1994; Petrosian & Donaghy 1999). It is also commonly believed that the observed relative abundances of ions in SEPs favor a SA model (e.g. Mason et al. 1986 and Mazur et al. 1992). More recent observations have confirmed this picture (see Mason et al. 2000, 2002, Reames et al. 1994 and 1997, and Miller 2003). One of the most vexing problem of SEPs has been the enhancement of ^3He in the so-called *impulsive or ^3He -rich events*, which sometimes can be 3 – 4 orders of magnitude above the photospheric value¹. There have been many attempts to explain this enhancement. Most of the proposed models, except the Ramaty and Kozlovsky (1974) model based on spallation (which has many problems), rely on resonant wave-particle interactions and the unique charge-to-mass ratio of ^3He (see e.g.

¹In addition there is charge-to-mass ratio dependent enhancement relative to the photospheric values of heavy ions in SEPs, and in few flares gamma-ray line emissions also points to anomalous abundance pattern of the accelerated ions (Share & Murphy 1998; Hua, Ramaty & Lingenfelter 1989). We will not be dealing with these anomalies in this paper.

Ibragimov & Kocharov 1977; Fisk 1978; Temerin & Roth 1992; Miller & Viñas 1993; Zhang 1995; Paesold, Kallenbach & Benz 2003). Most of these models assume presence of some particular kind of waves which preferentially heats ^3He ions to a higher temperature than ^4He ions, which then become seeds for subsequent acceleration by some (usually) unspecified mechanism (for more detailed discussion see Petrosian 2008). None of these earlier works did a compare model spectra with observations.

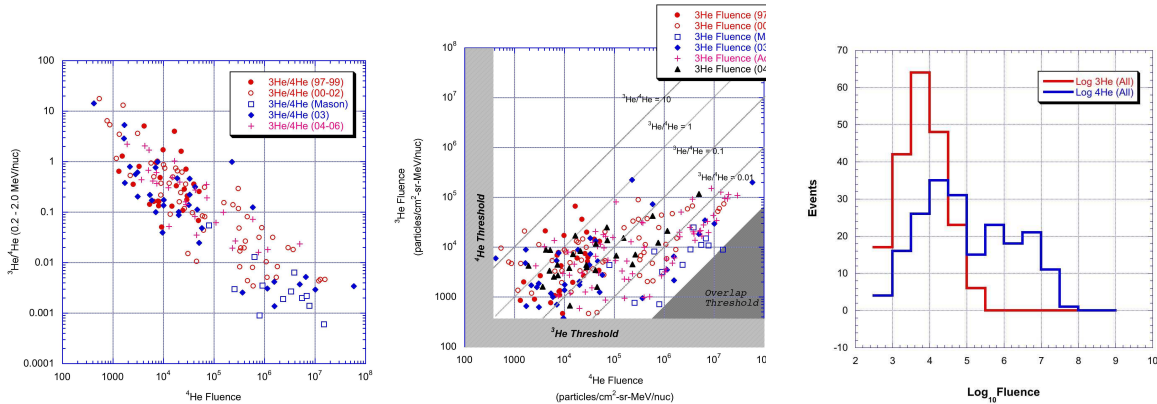


Fig. 1.— *Left:* Variation of the ratio of ^3He to ^4He fluences with the fluence of ^4He showing a continuum of enrichments and a strong anti correlation. *Middle:* ^3He vs ^4He fluences showing a much larger range for the latter while the former seems to be limited to a small range. Note that the ^3He fluences do not concentrate at the lower end which would be the case if observational threshold was affecting their distribution. *Right:* The distribution of fluences of ^3He and ^4He . Note that the high end of the ^4He distribution may be truncated because of the threshold of the fluence ratio (missing point in the lower left triangle of the middle panel) [From Ho05]. The fluences are in units of particles/(cm² sr MeV/nucleon).

In two more recent papers Liu, Petrosian & Mason 2004 and 2006 (LPM04, LPM06) have demonstrated that a SA model by parallel propagating waves can explain both the extreme enhancement of ^3He and can reproduce the observed ^3He and ^4He spectra. In LPM06 it was shown that the relative fluences of these ions, and to a lesser extent their spectral indexes, depend on several model parameters so that in a large sample of events one would expect some dispersion in the distributions of fluences and spectra. Ho et al. (2005; Ho05) analyzed a large sample of events and provide distributions of ^3He and ^4He fluences and the correlations between them. Our aim here is to explore the possibility of explaining these observations by the above mentioned dependence of the fluences on the model parameters. In particular we would like to explain the observations reproduced in Figure 1 which shows a strong anti correlation of $^3\text{He}/^4\text{He}$ ratio with ^4He fluence (left panel), but shows essentially no correlation between the two fluences (middle panel). More strikingly, the ^3He fluence distribution appears to be relatively narrow and follows a log-normal distribution, while ^4He distribution is much broader and may have a power law distribution in the middle of the range, where the observational selection effects are unimportant. Often the SEPs are

divided into two classes; impulsive-high enrichment and gradual-normal abundance classes. However, as evident from the left panel of the above figure there is a continuum of enrichment extending over many orders of magnitude.²

In the next section we describe some of the model characteristics that can explain these observations and in §3 we compare the model predictions with the observations, specifically the distributions of the fluences. A brief summary and conclusion is given in §4.

2. MODEL CHARACTERISTICS

The model used in LPM04 and LPM06 which successfully described the enrichment and spectra in several flares has several free parameters. As usual we have the plasma parameters density n , temperature T and magnetic field B_0 . It turns out that the final results are insensitive to the temperature as long as it is higher than 2×10^6 K (see Fig. 4 below), which is the case for flaring coronal loops. It also turns out that only a combination of density and magnetic field (\sqrt{n}/B_0) comes into play. We express this as the ratio of plasma to gyro-frequency of electrons, $\alpha = \omega_{pe}/\Omega_e$ which is related to the Alfvén velocity in unit of speed of light; $\beta_A = \delta^{1/2}/\alpha$, where $\delta = m_e/m_p$ is the ratio of the electron to proton masses. So in reality we have only one effective free plasma parameter α or β_A . On the other hand, several parameters are required to describe the spectrum of the turbulence. Following the above papers we assume broken power laws for the two relevant modes, the proton cyclotron (PC) and He cyclotron (HeC), with an inertial range $k_{\min} < k < k_{\max}$, and similar power law indexes q and q_h in and beyond the inertial range, respectively.³ The only difference between the two branches is that the wave numbers k_{\max} and k_{\min} for the PC mode are two times higher than those for the HeC mode. Finally there is the most important parameter related to the total energy density of turbulence, \mathcal{E}_{tot} , which determines both the rate of acceleration and, when integrated over the volume of the source region, determines the intensity or the strength of the event. This parameter is the characteristic time scale τ_p or its inverse the rate defined as (see, e.g. Pryadko & Petrosian 1997)

$$\tau_p^{-1} = \frac{\pi}{2} \Omega_e \left[\frac{4\bar{\mathcal{E}}_0}{B_0^2/8\pi} \right] \quad \text{with} \quad \bar{\mathcal{E}}_0 = \frac{(q-1)\mathcal{E}_{\text{tot}}}{(k_{\min}c/\Omega_e)^{1-q}}, \quad (1)$$

²The ⁴He distribution shows a weak sign of bi modality but this is not statistically significant. In this paper we will ignore this feature.

³In LPM06 we also have an index q_l describing the power law below the inertial range which is of minor consequence. For all practical purposes we can assume a sharp cutoff below k_{\min} which means $q_l \rightarrow \infty$.

for each mode. The factor of 4 arises from having two branches (PC and HeC) and two propagation directions of the waves (see LPM06 for details).

As shown in LPM04 and LPM06 papers the main difference between the acceleration process of ^3He and ^4He is in the difference between their acceleration rate or timescales (τ_a). The other relevant timescales, namely the loss (τ_{loss}) and escape (T_{esc}) times are essentially identical for the two ions (e.g. see left panel of Fig. 7 of LPM06). The acceleration timescales are different mainly at low energies (typically below one MeV/nucleon), where the acceleration time of ^4He is a longer (by one to two orders of magnitude). As a result at these low energies the ^4He acceleration time may be comparable or longer than the loss time which makes it difficult to accelerate ^4He ions. Most of ^4He ions are piled up below some energy (roughly where $\tau_a = \tau_{\text{loss}}$) and only a few of them accelerate into the observable range (e.g. see right panel of Fig. 7 of LPM06). However, because the acceleration times scale as τ_p while the loss time does not, for higher level of turbulence (larger $\bar{\mathcal{E}}_0$), the acceleration time may fall below the loss time so that ^4He ions can be then accelerated more readily (see Fig. 3 below). On the other hand, essentially independent of values of any of the above parameters, the ^3He acceleration time at all energies, in particular at low energies, is always far below its loss time so that in all cases (except for very high densities or very low values of τ_p^{-1}) ^3He ions are accelerated easily to high energies. The relative values of the escape and acceleration times (for both ions) determine their high energy spectral cutoffs.

Figure 2 shows variation with energy of acceleration times of ^3He (thick lines) and ^4He (thin lines) and their dependence on parameters k_{min} , α and q . The remaining parameters q_h and k_{max} only affect the slope of the low energy end of ^4He which does not affect the spectra noticeably. It is evident that the general behavior of the acceleration time scales described above (consisting of a low and a high energy monotonically increasing branches with a declining transition in between) is present in all models. These features change only quantitatively and often by small amounts. As expected lowering k_{min} decreases the acceleration times at the high energy branch (left panel). This is because the lower k_{min} waves interact resonantly with higher energy ions. On the other hand, a lower value of α (or larger Alfvén velocity or magnetization) decreases the times at the low energy branch (middle panel). Steeper spectra in the inertial range, produce a higher rate of acceleration (larger \mathcal{E}_0 ; see eq. [1]) and decrease the overall acceleration time scales (right panel)

Note that in this and subsequent figures, k_{max} is in units of Ω_p/c so that $k_{\text{max}} = 2\alpha\delta^{-1/2}$ in the labels means an actual $k_{\text{max}} = 2\Omega_p/v_A = \sqrt{2\beta_p}/r_{g,p}$, where $\beta_p = 2(v_{th,p}/v_A)^2$ is the plasma beta, and $v_{th,p} = k_B T/m_p$ and $r_{g,p} = v_{th,p}/\Omega_p$ are the proton thermal velocity and gyro radius. The scale of k_{max} is clearly beyond the MHD regime (where the wave frequency $\omega = v_A k \ll \Omega_p$), but is below the proton gyro radius for the chosen parameters

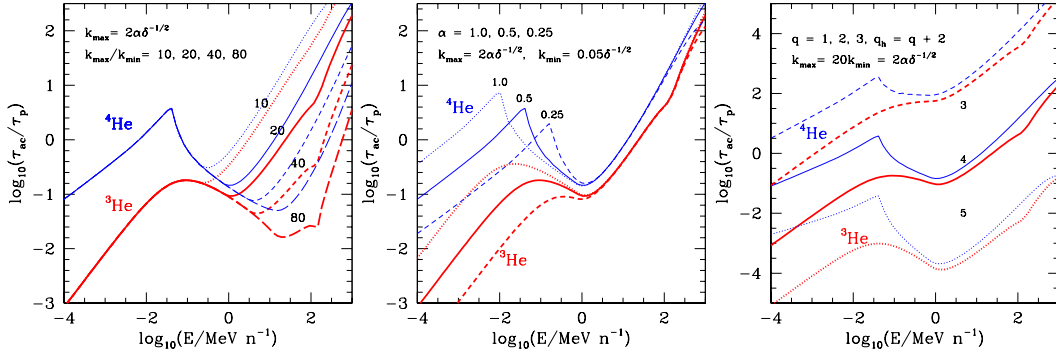


Fig. 2.— Dependence of the acceleration time of ^4He (thin, blue) and ^3He (thick, red) on k_{\min} (left), α (middle) and q (right). The lines are labeled with the corresponding numbers of each parameter. In each case the solid lines are for the fiducial model with $\alpha = 0.5$, $k_{\max} = 2\alpha\delta^{-1/2} = 10k_{\min}$, $q = 2$ and $q_h = 4$.

$$(\sqrt{2\beta_p} \sim 0.03).$$

Using these acceleration rates we calculate spectra of the two ions (as in LPM04 and LPM06) for a range of parameters. Figure 3 shows three sets of spectra where we vary k_{\min} , α and τ_p^{-1} . In each panel the solid lines are for the fiducial model ($\alpha = 0.5$, $k_{\max} = 2\alpha\delta^{-1/2} = 10k_{\min}$, $q = 2$ and $q_h = 4$) chosen to fit the spectra observed by *ACE/ULEIS* for 30 Sep. 1999 event. The spectral variations here reflect the above described variations of the acceleration timescales. Lower k_{\min} (or larger inertial range) yields a larger tail for both ions (left panel). Variation of α has a similar and smaller effect on ^3He spectra but it affects the ^4He spectra dramatically; for $\alpha \sim 1$ essentially there is no ^4He acceleration but the $\alpha \sim 1/4$ model accelerates a large number of ^4He ions beyond 0.1 MeV/nucleon and into the observable range (middle panel). This effect is even more pronounced for increasing values of τ_p^{-1} , where a factor of few increase in the general rate of acceleration (or the level of turbulence) causes a large increase of the fluence of ^4He (right panel), because, as stated above, its acceleration time becomes shorter than its loss time even at low energies. All these spectra show the same general characteristic features. While most ^3He ions are accelerated to high energies for essentially all model parameters appropriate for solar coronal conditions and reasonable level of turbulence, ^4He ions show a characteristic lower energy bump with a nonthermal hard tail. In general, the lower energy bump is below the observation range except for low α and high values of τ_p^{-1} . Since a high level of turbulence is expected for brighter and stronger events, this means that we get smaller $^3\text{He}/^4\text{He}$ flux or fluence ratios for brighter events. Note that the spectra in such cases may not agree with observations but this is not troublesome, because as is well established, the stronger events (the so-called gradual events) are associated with CMEs and shocks which most likely will modify the above spectra which are those of ions escaping the corona. Thus, the higher energy bumps

in the spectra shown here should be considered as seeds for such further acceleration during the transport from the lower corona to the Earth, which becomes more likely, and is expected to change the above spectra more significantly, for more energetic events. Thus if we give up the idea that there are two distinct classes of SEPs (impulsive and highly enriched and gradual and normal abundance) but that there is a continuum of events, which observations in Figure 1 show, then the above scenario implies that the main acceleration occurs in the solar corona. Subsequent interactions in CME shocks mainly modify the seed population escaping the turbulent coronal site.

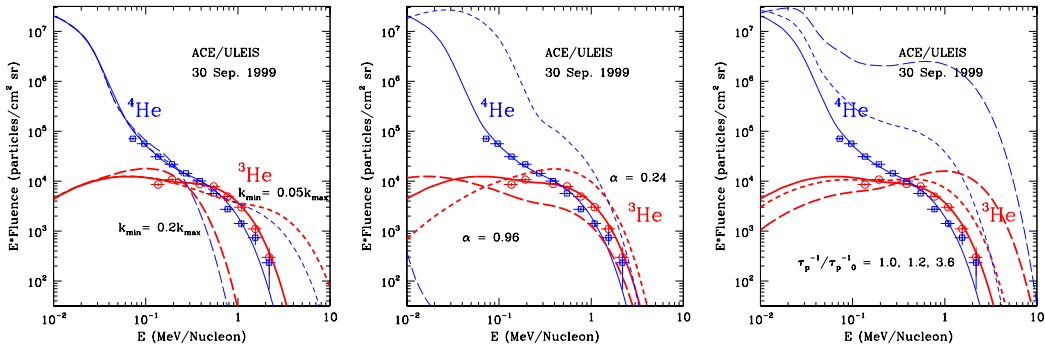


Fig. 3.— Dependence of the accelerated spectra of ^4He and ^3He on k_{\min} (left), α (middle) and τ_p^{-1} (right; τ_p^{-1} in units of $\tau_p^{-1,0} = 0.0055 \text{ s}^{-1}$). The lines are labeled with the corresponding numbers of each parameter. In each case the solid lines are for the fiducial model with $\alpha = 0.5$, $k_{\max} = 2\alpha\delta^{-1/2} = 10k_{\min}$, $q = 2$ and $q_h = 4$ that is chosen to fit the data point shown for the 30 Sep. 1999 event observed by *ACE*. Note that for a better indication what energy particles dominate the spectra in a log-log plot we plot particle energy time fluence.

From the spectra we can calculate the ratio of ^3He to ^4He fluences for different models which could be then compared with the observed ratios shown in Figure 1. Inspection of observed spectra indicate that a representative ion energy would be 1 MeV/nucleon. In Figure 4 we show the variation of this ratio with temperature (left panel) and τ_p^{-1} (middle and right panels) for several values of other important parameters. As evident this ratio is most sensitive to the value of τ_p^{-1} which represents the general rate of acceleration or the level of turbulence. The ratio can change from the highest observed value (~ 30) to near photospheric value ($\sim 2 \times 10^{-4}$) for only a factor of 30 change in τ_p^{-1} . It is natural to expect higher level of turbulence generation (i.e. a larger value of τ_p^{-1}) in stronger events. Therefore, this predicted correlation is in agreement with the general trend of observation shown in Figure 1 (left panel), if the strength of an event is measured by the observed fluence of ^4He ions and most other ions like carbon, nitrogen and oxygen.⁴ This seems reasonable

⁴It should be noted that while the observations are for fluences integrated from 0.2 to 2.0 MeV/nucleon

and calls for more quantitative comparison with observations and model prediction. In the next section we present one such comparison.

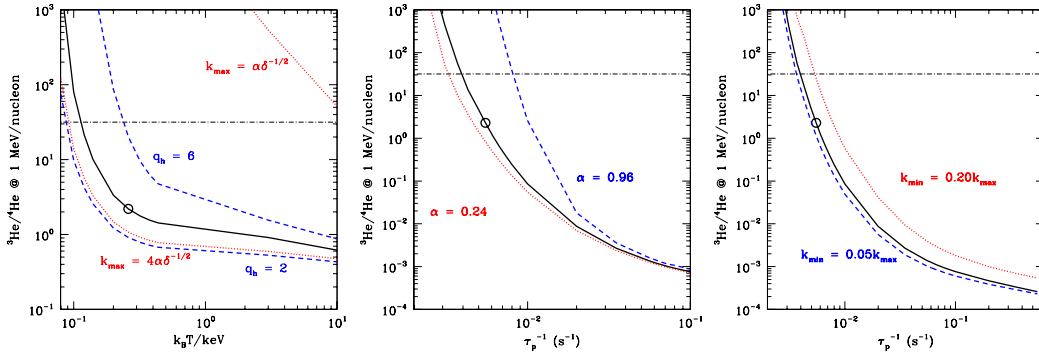


Fig. 4.— Variation of the accelerated ${}^3\text{He}$ to ${}^4\text{He}$ fluence ratio (at $E = 1$ MeV/nucleon) with background plasma temperature T (left) and τ_p^{-1} (middle and right) for several values of other specified model parameters. The lines are labeled with the corresponding numbers of each parameter. In each case the open circle stands for the model that fits spectra of the 30 Sep. 1999 event, and the solid lines are for the fiducial model with $\alpha = 0.5$, $k_{\max} = 2\alpha\delta^{-1/2} = 10k_{\min}$, $q = 2$ and $q_h = 4$. Note the weak dependence on the temperature for $T > 2 \times 10^6$ K and a strong dependence on τ_p^{-1} for all model parameters with saturates at chromospheric values of the ratio. The horizontal dot-dash line shows the highest ratio observed so far (see Fig. 1, left).

3. Distributions of Fluences

We have seen that the general observed behavior of the the ratio of the fluences defined as $R = F_3/F_4$ is similar to the model predictions. In this section we try to put this result on a firmer quantitative footing by considering the observed distributions of the fluences of both ions as shown in Figure 1 (right panel). Except for the minor truncation at high values of F_4 , the fluence of ${}^4\text{He}$, the observed distribution of F_3 , the fluences of ${}^3\text{He}$, seem to be almost bias free and not affected significantly by the observational selection effects. For example, there are well defined and steep decline both at the high and low fluences away from the peak ${}^3\text{He}$ value of $F_0 \sim 10^{3.7} \frac{\text{particles}}{\text{cm}^2\text{sr}(\text{MeV/nucleon})}$. This is not what one would expect if the data suffered truncation due to a low observation threshold. In such a case one would observe a distribution increasing up to the threshold followed by a rapid cutoff below it. Our model results described above also seem to predict the observed behavior. As stressed in previous section, the ${}^3\text{He}$ spectra and fluxes appear to be fairly independent of model parameters because essentially under all conditions most ${}^3\text{He}$ ions are accelerated and

our theoretical ratios are calculated at 1 MeV/ nucleon which is near the geometric or algebraic mean of the range.

form a characteristic concave spectrum. Thus we believe that it is safe to assume that the observed ${}^3\text{He}$ distribution is a true representation of the intrinsic distribution (as produced on the Sun). This distribution can be fitted very nicely with a log-normal expression.⁵ If we define the logs of the fluences and their ratio as

$$LF_3 \equiv \ln(F_3/F_0), \quad LF_4 \equiv \ln(F_4/F_0) \quad LR \equiv \ln R, \quad (2)$$

then from fitting the observed distribution of ${}^3\text{He}$ by a log-normal form we get:

$$\psi_3(LF_3) = \phi_0 \exp\left(\frac{LF_3}{\sigma_3}\right)^2 \quad \text{with} \quad \sigma_3 \sim 0.22, \quad (3)$$

which is shown on the right panel of Figure 5.

Using this distribution we now derive the distribution of ${}^4\text{He}$ fluences, $\psi_4(LF_4)$. For this we use the model predicted relationship between the two fluences as shown in Figure 4 above. We will use the two panels of this figure showing the dependence of the log of the fluence ratio LR on τ_p^{-1} . It turns out that most of these curves can be fitted by a simple function:

$$\ln(R/R_0) = LR - \ln R_0 = \frac{A}{\ln(\tau_p^{-1}/\tau_{p0}^{-1})}. \quad (4)$$

The left panel of Figure 5 shows fits to the curves in the right panel of Figure 4 with the indicated values of the fitting parameters A , R_0 and τ_{p0}^{-1} (which is not the same as the $\tau_{p,0}^{-1} = 0.0055\text{s}^{-1}$ in Fig. 3). We shall use this relation to transfer the ${}^3\text{He}$ fluences and distributions to those of ${}^4\text{He}$.

For a given value of τ_p^{-1} the number of events with ${}^4\text{He}$ log-fluences between LF_4 and $LF_4 + d(LF_4)$ (i.e. $\psi_4(LF_4)d(LF_4)$) is equal to $\psi_3(LF_3)d(LF_3)$, the number of events with ${}^3\text{He}$ log-fluence $LF_3 = LF_4 + LR(\tau_p^{-1})$ and $LF_3 + d(LF_3)$, where $d(LF_3) = d(LF_4)$ and $LR(\tau_p^{-1}) = \ln R_0 + A/\ln(\tau_p^{-1}/\tau_{p,0}^{-1})$. Thus we have

$$\psi_4(LF_4) = \psi_3(LF_4 + LR[\tau_p^{-1}]) = \phi_0 \exp\left(\frac{LF_4 + LR(\tau_p^{-1})}{\sigma_3}\right)^2 \quad (5)$$

However, we expect not a single value for τ_p^{-1} , which as stated above is a proxy for the strength of the event, but a broad distribution of events with different strengths, say $f(\tau_p^{-1})$.

⁵The truncation shown by the shaded area in the middle panel of Figure 1 introduces a slight bias against detection of low fluences. We estimate that, because there are fewer events at the high ${}^4\text{He}$ fluence end, this means a 10 to 20% underestimation of the distribution of the three lowest values of the ${}^3\text{He}$ histogram (right panel, Fig. 1). We will ignore this small correction, whose main effect is to increase the value of σ_3 by a small amount.

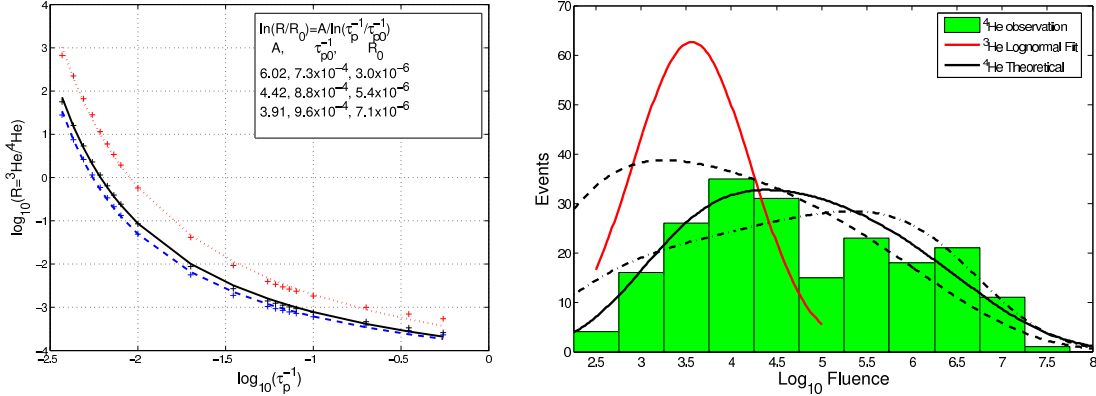


Fig. 5.— *Left:* A simple analytic fit (curves) to the model relations (points) between the fluence ratio and the acceleration rate or event strength represented by τ_p^{-1} for the three different values of k_{\min} of the right panel of Figure 4 with the indicated fitting parameters. *Right:* The fitted log-normal distribution to the ^3He fluences and predicted ^4He distributions of three models compared with observations. The solid line which gives the best fit is for $n = 2, k_{\min} = 0.1k_{\max}$, the dashed line is for $n = 2, k_{\min} = 0.2k_{\max}$ and the dash-dot line is for $n = 1.5, k_{\min} = 0.2k_{\max}$.

Since, as argued above, the ^3He fluence distribution $\psi_3(LF_3)$ is independent of τ_p^{-1} , then for a population of events we have

$$\psi_4(LF_4) = \int_0^\infty \phi_0 \exp\left(\frac{LF_4 + LR(\tau_p^{-1})}{\sigma_3}\right)^2 f(\tau_p^{-1}) d\tau_p^{-1}. \quad (6)$$

Every term in the above equations is determined by observations and our models except the distribution $f(\tau_p^{-1})$, which is a reflection of the level of the distribution of the level of turbulence and, when multiplied by the volume of the turbulent acceleration region (which does not affect the $^3\text{He}/^4\text{He}$ ratio), is related the overall strength of the event. Observations of solar flares show that most extensive characteristics which are a good measure of the flare strength or magnitude, such as X-ray, optical or radio fluxes, appear to obey a steep power law distribution, usually expressed as a cumulative distribution $\Phi(> F_i) \propto F_i^{-n}$ (or differential distribution $\phi(F_i) \propto F_i^{-n-1}$) with typically $n \sim 1.5$ (see, e.g. Dennis 1985 and reference therein). Such a distribution seems to roughly agree with the prediction of the so-called avalanche model proposed by Lu & Hamilton (1991). Now assuming that τ_p^{-1} also obeys such a power law distribution (i.e. $f(\tau_p^{-1}) \propto (\tau_p^{-1})^{-(n+1)}$) we can write the distribution of ^4He as:

$$\psi_4(LF_4) = \int_0^\infty \phi_0 \exp\left(\frac{LF_4 + \ln R_0 + A/x}{\sigma_3}\right)^2 e^{-nx} dx, \quad \text{with } x \equiv \ln(\tau_p^{-1}/\tau_{p0}^{-1}). \quad (7)$$

Using the above relations we have calculated the ^4He fluence distribution. The results for three models are compared with the observations on the right panel of Figure 5. Given the other model parameters (k_{\min}, α etc.) we have only one free parameter namely the index n for

this fit. The solid line obtained for the top curve of the left panel ($k_{\min} = 0.2k_{\max}, \alpha = 0.5$), and for $n = 2$ provides a good fit to the observed distribution of ${}^4\text{He}$ fluences. In order to demonstrate the sensitivity of the results to the parameters we also show two other model predictions based on slightly different parameter values. These results provide additional quantitative evidence (beside those given in LPM04 and LPM06) on the validity of the SA of SEPs by turbulence, and indicate that with this kind of analysis one can begin to constrain model parameters.

4. SUMMARY AND CONCLUSIONS

In this paper we have carried out further comparison between the prediction of models based on stochastic acceleration of SEP ions by turbulence. In our earlier works (LPM04, LPM06) we demonstrated that the extreme enrichments of ${}^3\text{He}$ and spectra of ${}^4\text{He}$ and ${}^3\text{He}$ observed in several events can be naturally described in such a model. Using the results based on this model, here we consider the relative distributions of ${}^4\text{He}$ and ${}^3\text{He}$ fluences derived from a large sample of event by Ho05. We show that with some simple and reasonable assumptions we can explain the general features of these observations as well.

These are clearly preliminary results and are intended to demonstrate that in addition to modeling only few bright events it is also important to look at population as a whole and ascertain that a model which can explain the detail characteristics of individual events can also agree with the distributions of observables for a large sample of events. Here we have shown how the dispersion in one parameter, namely the acceleration rate or the strength of the flare, can account for the observed distributions of fluences. The key assumption here is that the amount of produced turbulence (represented by τ_p^{-1}) has a wide dispersion and obeys a power law distribution similar to that observed for other extensive parameters that give a measure of the strength of a flare. The dispersion in other model parameters can also influence the final outcome. However, the dispersion of most of the other important parameters, like intensive parameters temperature, density and magnetic field, are expected to be much smaller than that of an extensive parameter like the overall strength of the event, the amount of turbulence produced, the flare volume etc. In addition, as shown in the previous section, the intensive parameters play a lesser role than the extensive parameter τ_p^{-1} in determining the relative characteristics of ${}^3\text{He}$ and ${}^4\text{He}$. Given the dispersion of any other parameter one may carry out similar integration over its range. However, for the reasons given above we expect smaller changes in the shapes of predicted distribution due to dispersion of most of the intensive parameters. Given a more extensive set of data such improvements may be needed can be carried out.

The existing data may be used to test some of our assumptions, in particular the assumption of constancy of the ^3He distribution. We intend to address these in future works. We can also make the above results more robust by using model fluences integrated over the same spectral range as the observations instead of fluences at 1 MeV/nucleon. One can also expand this approach and address the distributions of other characteristics besides the fluence, such as the spectral indexes or break energies (if any). The available data contain this information but require more analysis.

REFERENCES

- Dennis, B. R. 1985, *Sol. Phys.* 100, 465
- Fisk, L. A. 1978, *ApJ*, 224, 1048
- Hamilton, R. J., & Petrosian, V. 1992, *ApJ*, 398, 350
- Ho, G. C., Roelof, E. C., & Mason G. M. 2005, *ApJ*, 621, L141
- Liu, S., Petrosian, V., & Mason, G. M. 2004, *ApJ*, 613, L81
- Hua, X. M., Ramaty, R., & Lingenfelter, R. E. 1989, *ApJ*, 341, 516
- Liu, S., Petrosian, V., & Mason, G. M. 2006, *ApJ*, 636, 462
- Lu, E. T., & Hamilton, R. J. 1991, *ApJ*, 380, L89 2006, *ApJ*, 636, 462
- Mason, G. M., Mazur, J. E., & Dwyer, J. R. 2002, *ApJ*, 565, L51
- Mason, G. M., Mazur, J. E., Dwyer, J. R., Jokipii, J. R., Gold, R. E., & Krimigis, S. M. 2004, *ApJ*, 606, 555
- Mason, G. M., Ng, C. K., Klecker, B., & Green, G. 1989, *ApJ*, 339, 529
- Mason, G. M., Reames, D. V., Klecker, B., Hovestadt, D., & von Rosenvinge, T. T. 1986, *ApJ*, 303, 849
- Mason et al. 2002, *ApJ*, 574, 1039
- Masuda, S., Kosugi, T., Hara, H., Tsuneta, S., & Ogawara, Y. 1994, *Nature*, 371, 495
- Mazur, J. E., Mason, G. M., & Klecker, B. 1995, *ApJ*, 448, L53
- Miller, J. A. 1997, *ApJ*, 491, 939

- Miller, J. A. 2003, Multi-Wavelength Observations of Coronal Structure and Dynamics eds. Petrus C.H. et al. (COSPAR Colloquia Series Vol. 13), 387
- Miller, J. and Ramaty, R. 1987, Solar Physics 113, 195
- Miller, J. A., & Viñas, A. F. 1993, ApJ, 412, 386
- Möbius, E., Hovestadt, D., Klecker, B., & Gloeckler, G. 1980, ApJ, 238, 768
- Möbius, E., Scholer, M., Hovestadt, D., Klecker, B., & Gloeckler, G. 1982, ApJ, 259, 397
- Paesold, G., Kallenbach, R., & Benz, A. O. 2003, ApJ582, 495
- Park, B. T., Petrosian, V., & Schwartz, R. A. 1997, ApJ, 489, 358
- Petrosian, V., & Donaghy, T. Q. 1999, ApJ, 527, 945
- Petrosian, V., & Liu, S. 2004, ApJ, 610, 550 (PL04)
- Petrosian, V. 2008, To appear in ISSI workshop proceedings on Impulsive SEPs (2005,2006)
- Pryadko, J. M., & Petrosian, V. 1997, ApJ, 482, 774
- Ramaty, R. 1979, in Particle Acceleration Mechanisms in Astrophysics, eds. J. Arons, C. Max, & C. McKee (New York: AIP) 135
- Ramaty, R. & Kozlovsky, B. 1974, ApJ, 193, 729
- Reames, D. V., Meyer, J. P., & von Roseninge, T. T. 1994, ApJS, 90, 649
- Reames, D. V., Barbier, L. M., von Roseninge, T. T., Mason, G. M., Mazur, J. E., & Dwyer, J. R. 1997, ApJ, 483, 515
- Reames, D. V., & Ng, C. K. 2004, ApJ, 610, 510
- Reames, D. V., von Roseninge, T. T., & Lin, R. P. 1985, ApJ, 292, 716
- Share, G. H., & Murphy, R. J. 1998, ApJ, 508, 876
- Temerin, M., & Roth, I. 1992, ApJ, 391, L105
- Zhang, T. X. 1995, ApJ, 449, 916